John N. Rydberg, MSEE • Charlotte A. Hammond, MD • Roger C. Grimm, MS
Bradley J. Erickson, MD, PhD • Clifford R. Jack, Jr, MD • John Huston III, MD
Stephen J. Riederer, PhD

Initial Clinical Experience in MR Imaging of the Brain with a Fast Fluid-attenuated Inversion-Recovery Pulse Sequence[1]

PURPOSE: **To evaluate fast fluid-attenuated inversion-recovery (FLAIR) technique for imaging brain abnormalities.**

MATERIALS AND METHODS: **A fast FLAIR sequence was developed that provided 36 5-mm contiguous sections in 5 minutes 8 seconds. Resulting images were compared with dual-echo T2-weighted spin-echo images of 41 consecutive patients with brain abnormalities.**

RESULTS: **Contrast and contrast-to-noise ratios (C/Ns) (for contrast between the lesion and background and between the lesion and cerebrospinal fluid) for fast FLAIR exceeded the corresponding values for T2-weighted spin-echo images for all but the second-echo lesion-to-background C/N. Fast FLAIR provided equivalent or greater overall lesion conspicuity and enabled greater lesion detection in 98% and 100%, respectively, of the evaluations. Fast FLAIR images more often had image artifact, but this did not interfere with image interpretation in a significantly ($P \leq .05$) greater number of evaluations.**

CONCLUSION: **Fast FLAIR provides images that are superior to proton-density– and T2-weighted images for many image quality criteria.**

Index terms: Brain, abnormalities, 10.30, 10.781, 10.871 • Brain, MR, 10.121413 • Magnetic resonance (MR), pulse sequences

Radiology 1994; 193:173–180

[1] From the Magnetic Resonance Laboratory, Department of Diagnostic Radiology, Mayo Clinic and Foundation, 200 First St SW, Rochester, MN 55905 (J.N.R., C.A.H., R.C.G., B.J.E., C.R.J., J.H., S.J.R.); and the Department of Biomedical Engineering, University of Minnesota, Minneapolis (J.N.R.). Received February 28, 1994; revision requested April 19; revision received May 16; accepted May 20. Supported in part by grants CA 37993 and LM-07041 from the National Institutes of Health and Prevention. **Address reprint requests to** S.J.R.

CONVENTIONAL T2-weighted spin-echo (SE) magnetic resonance (MR) imaging has been a mainstay of evaluation of many pathologic processes of the brain (1). Most of these pathologic processes (eg, multiple sclerosis, infarction) increase the T2 relaxation times of the affected tissue, causing the lesion to have signal intensities intermediate between those of cerebrospinal fluid (CSF) and normal gray or white matter on T2-weighted images. This intermediate signal intensity usually necessitates the acquisition of both T2- and proton density–weighted images for accurate interpretation, particularly when these lesions abut a CSF border.

A technique called fluid-attenuated inversion-recovery (FLAIR) (Picker, Cleveland, Ohio) (2–4), and its variations (5,6), has been demonstrated at 1.0 T. This method produces heavily T2-weighted CSF-nulled images by coupling an inversion pulse followed by long inversion time (TI), to a long-echo-time (TE) readout. With nulling of the CSF, a tissue abnormality usually becomes the brightest object in these images, thereby enhancing its conspicuity. Furthermore, while the length of the TE used in T2-weighted SE imaging is limited by the increasing artifact and partial voluming effects of CSF as the TE is increased (2–7), these longer TEs can be used in FLAIR, and images can thus be acquired with greater T2 weighting, because the CSF signal is nulled out. However, although FLAIR has had great success in displaying lesions not seen with conventional T2-weighted SE sequences (3,4,7), it has been limited by long acquisition times caused by the long TIs and repetition times (TRs) required to both null CSF and allow non-CSF tissues adequate signal recovery before readout. For example, 13 minutes is required to obtain 10 sections with a resolution of 128 × 256 with use of a 6,000/160/2,100 (TR msec/TE msec/TI msec) sequence (3).

One solution to improve the imaging efficiency of FLAIR, the use of a RARE (rapid acquisition with relaxation enhancement) readout (8) (recently implemented as fast SE [9,10]), was originally demonstrated by acquisition of three or four echoes per excitation (2,6). While this implementation provided a moderate improvement in imaging efficiency, the use of a nonselective inversion pulse limited the amount of acquisition time that provided useful CSF attenuation. A more recent implementation of FLAIR-RARE typically acquires 16 echoes per excitation (11). This method produces a more substantial improvement in imaging efficiency but lacks complete CSF suppression because it uses a TI that does not null CSF.

The purpose of this work was to develop a sequence for performing FLAIR imaging with increased section efficiency and to evaluate this expedited technique for imaging multiple abnormalities of the brain. This resulting technique, referred to as fast FLAIR, provides 36 5-mm-thick contiguous sections in 5 minutes 8 seconds. The fast FLAIR images were compared with early- and late-echo images of a conventional T2-weighted SE imaging sequence in 41 consecutive patients with brain abnormalities. The comparison was based on measures of contrast, contrast-to-noise ratio (C/N), lesion conspicuity, lesion detection, and image artifact.

MATERIALS AND METHODS

Fast FLAIR Pulse Sequence

The technical goal of this work was to reduce the overall imaging time while still acquiring high-quality FLAIR images of a

Abbreviations: C/N = contrast-to-noise ratio, CSF = cerebrospinal fluid, FAISE = fast-acquisition interleaved spin echo, FLAIR = fluid-attenuated inversion recovery, RARE = rapid acquisition with relaxation enhancement, SE = spin echo, S/N = signal-to-noise ratio, TE = echo time, TI = inversion time, TR = repetition time.

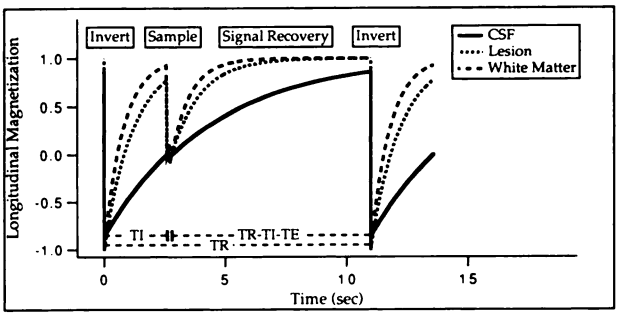

1.

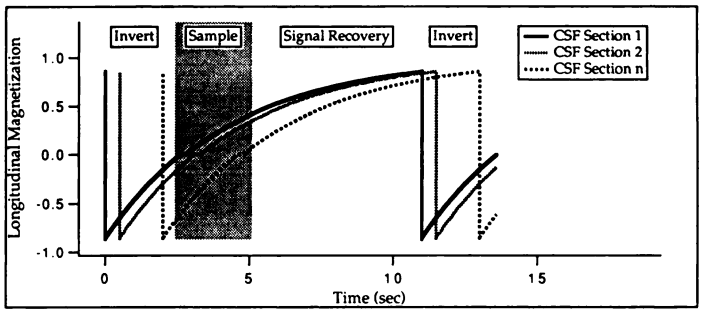

2a.

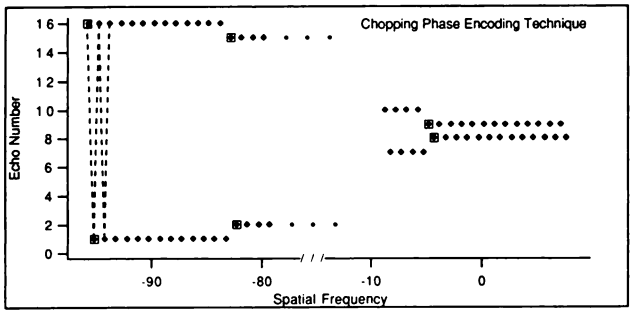

3.

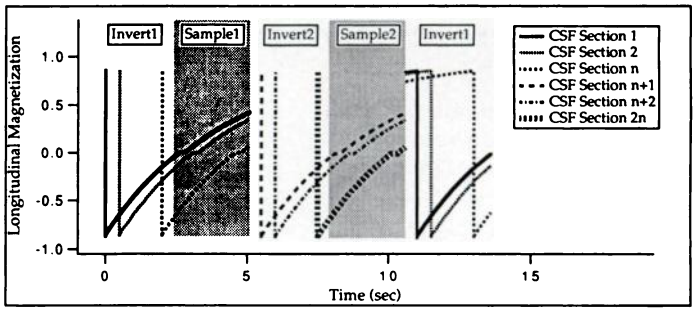

2b.

Figures 1–3. **(1)** FLAIR sequence with acquisition of one section per TR. The section is inverted, the TI delay allows the CSF signal to null, the section is sampled, and the signal recovery delay ($\approx$ TR − TI − TE) allows longitudinal magnetization recovery of all intracranial contents. **(2)** Multisection diagrams of **(a)** FLAIR (with use of section-selective inversion pulses) and **(b)** fast FLAIR, the sequence resulting from this work. In fast FLAIR, the signal recovery delay ($\approx$ TR − TI − TE), previously used only for longitudinal signal recovery, is used to invert and sample an additional group of sections (n + 1 to 2n), thereby potentially doubling section/time efficiency. **(3)** Chopping phase-encoding technique used in fast FLAIR, with echoes from the first excitation contained in boxes. This phase-encoding scheme alternates echoes 1 and 16 at the highest (most negative here) spatial frequencies and echoes 2 and 15 at the next highest spatial frequencies. This scheme is repeated (ie, echoes 3 and 14, echoes 4 and 13) until echoes 8 and 9 are alternated at the lowest (near zero) spatial frequencies. Broken lines illustrate the alternating of echoes across k space. This phase-encoding technique was found to be the most effective phase-encoding scheme compared with four other possible options.

volume encompassing the entire brain. To accomplish this goal, two techniques were incorporated: (*a*) acquisition of additional sections during the signal recovery delay, a method we call "sequential interleaving"; and (*b*) the use of an increased number of phase encodings per repetition (RARE). As part of the RARE implementation, a specific 16-echo phase-encoding technique was used.

The fast FLAIR signal characteristics are given by the following inversion recovery equation (12): Signal = $k(1 - 2e^{-TI/T1} + e^{-TR/T1})e^{-TE_{eff}/T2}$, where k is a proportionality constant including proton density and TE_{eff} is the effective TE of the RARE readout, assumed to be small compared with TR. Also, it is assumed that the longitudinal magnetization developed during the RARE readout has a negligible effect on the recovered longitudinal magnetization at the end of the repetition. These assumptions are valid for the large TR (11,000 msec) used. With a TI of 2,600 msec, which was found to consistently null CSF signal at the 11,000-msec TR used in the studies reported here, this equation numerically results in a T1 of 4,200 msec for CSF, consistent with recently published values (13). Because FLAIR is fundamentally an inversion recovery sequence, the degree of T1 saturation, given by the term in parentheses in the equation, is dictated primarily by the TI. Unlike a typical partial saturation/SE sequence, the TR of FLAIR sequences should not be used as a measure of T1 saturation. In fact, for the TR/TI times used in this study, the degree of recovery of longitudinal magnetization of non-CSF materials immediately before readout was comparable to or less than that of the T2-weighted sequences used.[2] That is to say, the degree of contamination of the desired signal by T1 effects was comparable or worse in the FLAIR sequence than in the sequences to which it was being compared.

Sequential interleaving.—As a reference, a single-section version of FLAIR is shown in Figure 1. Shown in this plot are the longitudinal magnetizations M_z for white matter (T1 = 790 msec [14]), a lesion with a T1 of 1,200 msec, and CSF (assumed T1 of 4,200 msec). After application of the inversion pulse, the TI delay allows non-CSF tissue to attain substantial longitudinal magnetization recovery while still nulling the CSF. At the TI that nulls the CSF signal, sampling of this longitudinal magnetization is performed by the standard 90°–180° pulse pair. At a TE typically exceeding 100 msec (to provide T2-dependent weighting) a single phase encoding is sampled. After this sampling, a signal recovery delay ($\approx$ TR − TI − TE) is used to permit recovery of all intracranial contents to nearly full magnetization.

Shown in Figure 2 are multisection schematics of the original FLAIR sequence with use of a section-selective inversion pulse and the expedited fast FLAIR version. For purposes of clarity, this figure presents only the longitudinal magnetization of the CSF signal with use of the acquisition parameters of Figure 1. In the original FLAIR acquisition (Fig 2a), only the TI delay is used to invert additional sections before the signal from the first section is sampled. In the fast FLAIR sequence (Fig 2b), not only is the TI delay used to excite multiple sections per TR, but the signal recovery delay ($\approx$ TR − TI − TE) is also used for data acquisition. This technique, previously used in a standard inversion recovery sequence (15), potentially doubles the number of sections imaged for the same amount of imaging time and henceforth will be called "sequential interleaving."

[2] With use of a Bloch equation simulation, it was determined that compared with the dual-echo SE sequence with the poorest longitudinal signal recovery used in this study (2,000/30, 80), the fast FLAIR sequence maximally has 1.6% more absolute longitudinal magnetization for tissues with a T1 of approximately 680 msec, equivalent longitudinal magnetization for tissues with T1s on the order of 980 msec, and less longitudinal magnetization recovery for tissues with a T1 greater than 1,000 msec—a T1 range often assumed for abnormality. Compared with T2-weighted sequences with a TR of more than 2,000 msec, the relative amount of T1 weighting in fast FLAIR becomes even worse.

RARE readout.—To reduce acquisition time, 16 phase-encoding views were measured per repetition. The specifics of the phase-encoding scheme used were driven by several factors. First was the desire for a TE_{eff} in the 130–160-msec range previously used for FLAIR (3). Second, to maintain an adequate signal-to-noise ratio (S/N), the signal was acquired at the same bandwidth, ±16 kHz, used for the early echo of the standard SE images. This bandwidth choice resulted in 17-msec interecho spacing.

Five phase-encoding techniques were considered for use in fast FLAIR. The first two phase-encoding techniques considered were 136- and 153-msec TE_{eff} versions of the fast-acquisition interleaved SE (FAISE) phase-encoding technique (10). Also considered were two "sequential" phase-encoding techniques (9,16), one with a TE_{eff} of 145 msec and the second with a TE_{eff} of 136 msec. Figure 3 displays the fifth phase-encoding technique considered, henceforth called "chopping," which is a 16-echo variation of a phase-encoding technique previously shown to have decreased sensitivity to flow artifacts (17,18). The chopping phase-encoding scheme alternates echoes 1 and 16, 2 and 15, 3 and 14, . . ., 8 and 9 across frequency space. This phase-encoding technique requires acquisition of 16 additional frequency (k) space lines, an extended field of view (no phase wrap), and a half-Fourier reconstruction technique (19,20) to force the ghosts that result from the rapid alternating of the echoes outside the primary image. Since the eighth and ninth echoes are alternated at the center of frequency space, the region that dictates overall image contrast (21), the contrast of this image is considered to be the average of these TEs, or 145 msec.

The choice of phase-encoding technique was based on the ability of each technique to suppress blurring and ghosting artifacts seen along the phase-encoding direction in RARE (9) and FLAIR (5) acquisitions. The amount of image blurring and/or image ghosting seen in RARE acquisitions is dependent on the k space ordering of the echoes, blurring being more relevant for these phase-encoding techniques. Typically only ghosting artifacts, caused by inflow of nonnulled CSF into sections with high CSF flow rates, are observed in FLAIR images. These flow artifacts still occur despite doubling the inversion section thickness to minimize the inflow (3).

Each phase-encoding technique was evaluated on each of five volunteers with use of the same imaging parameters used on patients. The five phase-encoding techniques were qualitatively evaluated by two experienced readers on the basis of object edge definition and presence of ghosting artifact. They were also evaluated quantitatively by using standard deviations of noise measured in large regions of interest placed outside the head along the phase-encoding (22) and the frequency-encoding directions. The latter were measured to normalize for differences in frequency space sampling.

Patient Studies

All examinations were performed on a 1.5-T imager (Signa; GE Medical Systems, Milwaukee, Wis). All dual-echo T2-weighted SE and fast FLAIR images were obtained in the axial plane with use of a standard quadrature head coil and inferior spatial presaturation. Patients were imaged with a dual-echo conventional T2-weighted SE sequence with the following parameters: first-echo TE of 30 msec with ±16-kHz bandwidth, second-echo TE of 80 msec with ±8-kHz bandwidth, one acquisition, 192 × 256 resolution, and gradient moment nulling in the section-select and readout directions. The TR, adjusted to obtain the desired number of sections, ranged from 2,000–2,500 msec; corresponding acquisition times ranged from 6 minutes 48 seconds to 8 minutes 30 seconds. Fast FLAIR images, as previously described, were also acquired with use of the chopping phase-encoding technique, an inversion width approximately twice the section width (3), and the following parameters: $TR/TE_{eff}/TI$ = 11,000/145/2,600, 16 echoes per repetition, 256 × 192 spatial resolution, and one dummy repetition (a cycle not sampled but used to bring the longitudinal magnetization to equilibrium). Eighteen sections were imaged in each 2-minute 34-second acquisition time with use of two nine-section groups. For each patient, two acquisitions of the fast FLAIR sequence were concatenated, providing images from 36 contiguous 5-mm-thick sections in 5 minutes 8 seconds. Odd-numbered sections were imaged in the first acquisition and even sections in the second acquisition.

Forty-one patients with brain abnormalities were consecutively imaged as the schedule permitted from July to October 1993 according to the described protocol; one additional study was eliminated owing to extreme patient motion that caused the study to be nondiagnostic with all sequences used. The age range of the 41 successfully imaged patients was 6–80 years, with a mean and standard of deviation of 52 years ± 21. The patients' pathologic conditions included infarction (n = 15), small vessel ischemia or infarction (n = 11), multiple sclerosis or other demyelinating disorder (n = 9), and miscellaneous other conditions (n = 6: inflammation, n = 3; meningioma, n = 1; olivopontocerebellar atrophy, n = 1; human immunodeficiency virus infection of the brain, n = 1). Owing to the lack of verification by means of biopsy, all diagnoses are the present working hypotheses based on clinical history, clinical presentation, and imaging studies.

Evaluation of Patient Studies

First- and second-echo images from the T2-weighted SE sequence were each compared with the fast FLAIR images with four quantitative and three qualitative criteria. The four quantitative criteria were lesion-to-background contrast, lesion-to-background contrast-to-noise ratio (C/N), lesion-to-CSF contrast, and lesion-to-CSF C/N. "Background" was defined as the normal brain (non-CSF) parenchyma adjacent to the lesion, typically white matter. The three qualitative criteria were lesion conspicuity, lesion detectability, and image artifact.

To prevent the quantitative results from one study dominating the overall averages of the contrast and C/N measurements, a maximum of two representative, randomly chosen lesions were measured from every patient study. Lesions were selected randomly from one of the sequence types, starting from the most inferior section and progressing superiorly until the first lesion was detected that was seen on the other two sequence types at the same location. This was then repeated for the same patient study but starting superiorly and proceeding inferiorly. This procedure randomized the relative position at which lesions were selected and ensured that lesions were selected from inferiorly located sections, where fast FLAIR images were susceptible to flow artifacts. For all images, mean lesion signal was measured within a region of interest placed within similar uniform areas of the targeted lesion. Mean background signal intensity was measured in areas immediately surrounding the lesion. The standard deviation of the noise was measured along the phase-encoding direction in regions outside the head. Lesion-to-background contrast was defined as the difference between the signals of lesion and background divided by the background signal. Lesion-to-background C/N was calculated by dividing the difference between lesion and background signals by the standard deviation of the image noise. Similar procedures were used in determining lesion-to-CSF contrast and C/N. A total of 73 lesions from the 41 patients studied was analyzed. For nine of the studies, only one lesion fit the selection criteria; for the other studies, two lesions were evaluated.

Because numerical contrast and C/N values for any sequence type can cover a broad range over the number of studies used, sequence performance was compared on a lesion-by-lesion basis with use of relative contrast and C/N values. The ratio of relative lesion-to-background contrast on fast FLAIR images to that on first-echo T2-weighted SE images was determined: a ratio exceeding unity indicates superior performance of fast FLAIR for that lesion, and a value less than unity indicates inferior performance of fast FLAIR. Similar ratios were determined for lesion-to-background C/N and lesion-to-CSF contrast and C/N for each lesion. Similar ratios were determined for fast FLAIR versus second-echo T2-weighted SE images. The statistical significance of quantitative data was determined by using a paired t test (23, p 250–254) with Bonferonni correction (24).

The qualitative analysis was performed as follows. For each patient study, the combined data set from first- and second-echo SE images was evaluated and compared with the fast FLAIR image set inde-

pendently by four experienced neuroradiologists (C.A.H., B.J.E., L.R.J., J.H.). Owing to the intersequence patient head movement periodically seen when comparing SE and fast FLAIR sections, and because contiguous sections could be acquired in less time with fast FLAIR, all fast FLAIR sections were compared with all SE sections. The evaluation was unblinded because of obvious differences in CSF signal intensity. The following scale was used to evaluate lesion conspicuity, defined as ease of lesion visualization; lesion detection, defined as the presence or absence of lesions; and overall image artifact: +1 = fast FLAIR superior to SE imaging, +0 = fast FLAIR comparable to SE imaging, −1 = fast FLAIR inferior to SE imaging.

Each evaluator was also asked to quantify the number of additional lesions seen on images obtained with the superior sequence for lesion detection (on a scale of 1, 2, or ≥3) and to indicate whether image artifact interfered with the interpretation of either type of image. To partially correct for obvious sampling differences in acquiring contiguous 5-mm fast FLAIR versus 5-mm SE sections with 2.5-mm intersection gap, the evaluators were asked to subjectively estimate what percentage of additional lesions they believed were detected because of this sampling difference. The statistical significance of qualitative data was determined with a sign test (23, pp 295–299).

RESULTS

Phase-encoding Selection

Qualitatively, both readers judged the chopping phase-encoding technique to be superior to both sequential phase-encoding techniques in all five volunteers and superior to both FAISE phase-encoding techniques in four of the five volunteers. In the remaining volunteer, one reader rated both FAISE phase-encoding techniques to be equivalent to the chopping phase-encoding technique, while the other rated only the 153-msec-TE FAISE phase-encoding technique to be equivalent. The chopping phase-encoding technique was found to be quantitatively superior to all other phase-encoding techniques in all volunteers except in one, in whom the sequential (TE = 136 msec) phase-encoding technique was found to be essentially equivalent. Because the chopping phase-encoding technique was found to be superior or equivalent to the other four phase-encoding techniques both qualitatively and quantitatively, it was chosen as the phase-encoding technique for the patient studies.

Quantitative Patient Results

Lesion-to-background contrast measurements and C/Ns for all 73 lesions analyzed are summarized in Table 1. Presented separately are the ratios for mean contrast and C/N for fast FLAIR images to those of first- and second-echo SE images for each pathology group and for the composite study. The lesion-to-background contrast of fast FLAIR is more than four times greater than that of first-echo SE imaging for the multiple sclerosis group and more than five times greater for the other groups. Overall, contrast was found to be significantly greater for fast FLAIR than first-echo SE imaging at $P < .001$. Likewise, the C/N performance of fast FLAIR significantly exceeded that of first-echo imaging at $P < .001$. Compared with second-echo SE imaging, fast FLAIR consistently displayed 75% higher lesion-to-background contrast, which was significant at the $P < .001$ level. The lesion-to-background C/N of fast FLAIR is approximately 12% worse than that of second-echo SE imaging ($P < .01$), which is expected due to differences in bandwidth alone. This lost C/N could conceivably be regained if the bandwidth used for fast FLAIR were somewhat reduced, with the penalty of a modest increase in acquisition time.

Lesion-to-CSF C/N and contrast results are also summarized in Table 1. Lesion-to-CSF C/Ns for fast FLAIR were 2.26 ± 0.09 and 3.3 ± 0.4 (mean ±

Table 1
Lesion-to-Background and Lesion-to-CSF Relative Contrast and C/N: Fast FLAIR versus First- and Second-Echo T2-weighted SE Imaging

Patient Group	No. of Patients/ No. of Lesions	Fast FLAIR vs First Echo		Fast FLAIR vs Second Echo	
		Contrast	C/N	Contrast	C/N
		Lesion-to-Background*			
Infarct	15/25	5.64 ± 0.45	1.72 ± 0.19	1.75 ± 0.12	0.86 ± 0.07
Multiple sclerosis	9/17	4.39 ± 0.46	1.31 ± 0.18	1.77 ± 0.17	0.88 ± 0.09
Small vessel ischemia/ infarct	11/21	5.33 ± 0.26	1.51 ± 0.08	1.98 ± 0.10	0.91 ± 0.04
Miscellaneous	6/10	5.08 ± 0.61	1.68 ± 0.34	1.75 ± 0.15	0.86 ± 0.10
Composite	41/73	5.17 ± 0.22†	1.55 ± 0.09†	1.84 ± 0.07†	0.88 ± 0.04‡
		Lesion-to-CSF§			
Infarct	15/25	30 ± 5	2.2 ± 0.2	59 ± 18	3.4 ± 0.8
Multiple sclerosis	9/17	39 ± 6	2.2 ± 0.2	72 ± 14	3.0 ± 0.5
Small vessel ischemia/ infarct	11/21	45 ± 9	2.3 ± 0.2	94 ± 15	3.1 ± 0.7
Miscellaneous	6/10	57 ± 9	2.6 ± 0.2	85 ± 19	3.6 ± 0.7
Composite	41/73	38 ± 4†	2.26 ± 0.09†	75 ± 11†	3.3 ± 0.4†

Note.—Displayed are the numeric averages and the standard deviations of the mean.
* Absolute values for fast FLAIR contrast and C/N were 1.15 ± 0.05 and 20.29 ± 0.81, respectively.
† Values for fast FLAIR significantly larger than those for T2-weighted SE imaging at $P = .001$ level.
‡ Values for fast FLAIR significantly smaller than those for T2-weighted SE imaging at $P = .01$ level.
§ Absolute values for fast FLAIR contrast and C/N were 14.67 ± 1.00 and 35.27 ± 1.03, respectively.

Table 2
Lesion Conspicuity and Lesion Detection for the 41 Patient Studies

Radiologist	Fast FLAIR Superior (+1)	Fast FLAIR = T2-weighted SE (0)	T2-weighted SE Superior (−1)	Mean
	Lesion Conspicuity			
1	35	5	1	+0.83 ± 0.07*
2	38	3	0	+0.93 ± 0.04*
3	24	15	2	+0.54 ± 0.09*
4	33	8	0	+0.80 ± 0.06*
Total	130	31	3	+0.77 ± 0.04*
	Lesion Detection			
1	20	21	0	+0.49 ± 0.08*
2	27	14	0	+0.66 ± 0.07*
3	17	24	0	+0.41 ± 0.08*
4	22	19	0	+0.54 ± 0.08*
Total	86	78	0	+0.52 ± 0.04*

Note.—Displayed are the numeric averages and the standard deviations of the mean.
* Fast FLAIR significantly superior to T2-weighted SE imaging at $P = .0001$ level.

Table 3
Overall Assessment of Artifact on Fast FLAIR and T2-weighted SE Images

Radiologist	Fast FLAIR Less Artifact (+1)	Fast FLAIR = T2-weighted SE (comparable artifact)(0)	T2-weighted SE Less Artifact (−1)	Mean
1	4	17	20	−0.39 ± 0.10*
2	2	8	31	−0.71 ± 0.09*
3	1	37	3	−0.05 ± 0.05†
4	2	6	33	−0.76 ± 0.08*
Total	9	66	87	−0.48 ± 0.05*

Note.—Displayed are the numeric averages and the standard deviations of the mean.
* Fast FLAIR statistically inferior to T2-weighted SE at $P = .005$ level.
† Not statistically significant at $P = .05$ level.

Table 4
Assessment of Interpretation-interfering Artifact on Fast FLAIR and T2-weighted SE Images

Radiologist	T2-weighted SE Artifact Interference (+1)	Fast FLAIR Artifact Interference (−1)	Net Artifact Interference
1	4	8	−0.10 ± 0.08*
2	2	6	−0.10 ± 0.07*
3	1	2	−0.02 ± 0.04*
4	2	9	−0.17 ± 0.08*
Total	9	25	−0.10 ± 0.03*

Note.—Displayed are the numeric averages and the standard deviations of the mean.
* Not statistically significant at the $P = .05$ level.

standard deviation of the mean) times greater than those for first- and second-echo SE images, respectively. Fast FLAIR images had 38 ± 4 and 75 ± 11 times greater contrast than the first- and second-echo images, respectively. Overall study CSF S/Ns of 3.4 ± 0.3, 62 ± 2, and 71 ± 2 (mean ± standard deviation of the mean) were measured for fast FLAIR, first-echo SE, and second-echo SE imaging, respectively. The similarity of the noise and fast FLAIR CSF signal intensities caused the fast FLAIR CSF signal intensity to vary greatly and resulted in the large variations seen in the relative contrast measurements.

Qualitative Analysis

Results of the qualitative comparisons of fast FLAIR with conventional long TR SE imaging are summarized in Tables 2–4 for lesion conspicuity, lesion detection, and image artifact. In all cases, pooled and individual results are shown for all four neuroradiologists. For lesion conspicuity (Table 2), fast FLAIR received an overall score of +0.77 ± 0.04 (mean ± standard deviation of the mean) and was judged superior or comparable to the T2-weighted SE examination in all but three evaluations, each of which came from separate studies. Lesion conspicuity with fast FLAIR was found to be significantly superior to that with T2-weighted SE imaging at the $P = .0001$ level for each neuroradiologist and for the pooled results. All neuroradiologists rated fast FLAIR comparable or superior to T2-weighted SE imaging for lesion detection in all cases (Table 2). Fast FLAIR received an overall lesion detection score of +0.52 ± 0.04 (mean ± standard deviation of the mean) and was found to be statistically superior to T2-weighted SE imaging at the $P = .0001$ level for each neuroradiologist and for the pooled results. On average, the neuroradiologists found that fast FLAIR enabled detection of 1.1 ± 1.2 more lesions per study than the T2-weighted SE acquisitions and subjectively estimated that less than one-third of these additional detections were caused by differences in section sampling (5-mm contiguous sections for fast FLAIR vs 5-mm sections with 2.5-mm intersection gap for T2-weighted SE imaging).

For overall image artifact (Table 3), fast FLAIR received an overall score (mean ± standard deviation of the mean) of −0.48 ± 0.05 and was rated inferior to the T2-weighted SE examination by three of the four neuroradiologists at a statistically significant level ($P = .005$). However, when fast FLAIR was compared with SE imaging regarding the incidence of artifact that could potentially interfere with image interpretation, fast FLAIR was not found to be significantly different ($P = 0.05$) than T2-weighted SE imaging for any individual neuroradiologist or for the composite results (Table 4). When present, artifacts tended to occur in areas of prominent CSF pulsatility, such as inferiorly located sections and sections containing foramina of the CSF ventricular system. These locations also tended to be sites of incomplete CSF nulling, if present. These findings were believed to result from inflow of nonnulled CSF into sections of interest between the inversion pulse and beginning of signal sampling and have previously been noted in FLAIR images (5).

Patient Studies

Sample images from the four patient groups are shown in Figures 4–7. Figure 4 shows images of a patient with an infarction, visible on fast FLAIR sections but not any of the T2-weighted SE images. Figure 5 demonstrates increased lesion conspicuity seen with the fast FLAIR sequence in a patient with multiple sclerosis. Figure 6 shows images of a patient with small vessel ischemia and the dramatic improvement in lesion conspicuity that resulted from CSF nulling. Also seen is an additional lesion in the left frontal lobe that was detected only with fast FLAIR. Figure 7c shows a meningioma on a fast FLAIR image, also seen on the next cephalic fast FLAIR section, that was seen only retrospectively on T2-weighted SE images due to the similar T2 signal. The meningioma is also seen in Figure 7d, a T1-weighted SE image enhanced with contrast medium.

DISCUSSION

MR imaging of the brain has been demonstrated with use of an accelerated or fast version of a FLAIR pulse sequence. The original FLAIR sequence provided 10 CSF-suppressed sections with contrast characteristics otherwise similar to those of conventional long TR SE imaging in 13 minutes (3). In this work, interleaving of two sections (sequential interleaving) and a 16-echo RARE readout were incorporated to improve the efficiency (sections imaged per unit time) of the FLAIR sequence. With these two enhancements the fast FLAIR sequence developed was able to image 36 contiguous 5-mm-thick sections in an acquisition time of 5 min-

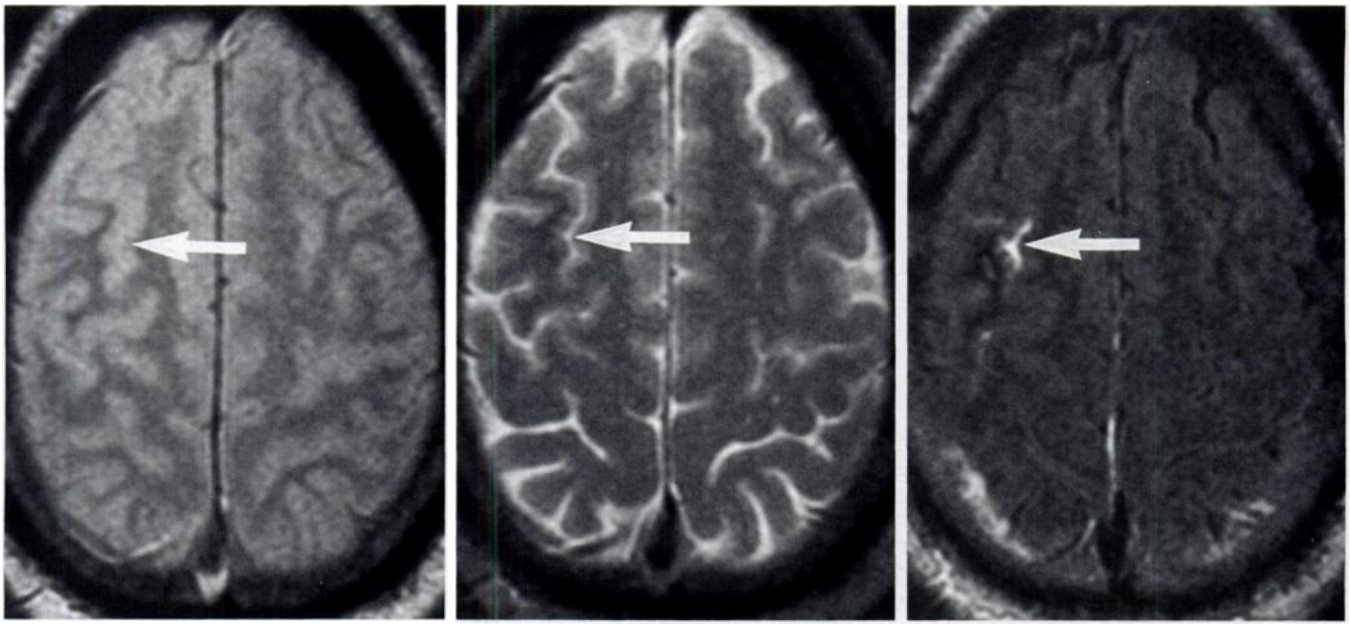

a. b. c.

Figure 4. Infarction. **(a, b)** Conventional SE images (2,350/30, 80) do not show the lesion. **(c)** Fast FLAIR image (11,000/145/2,600). Arrow = infarct. Increased signal intensity was also visible on the previous caudal fast FLAIR section.

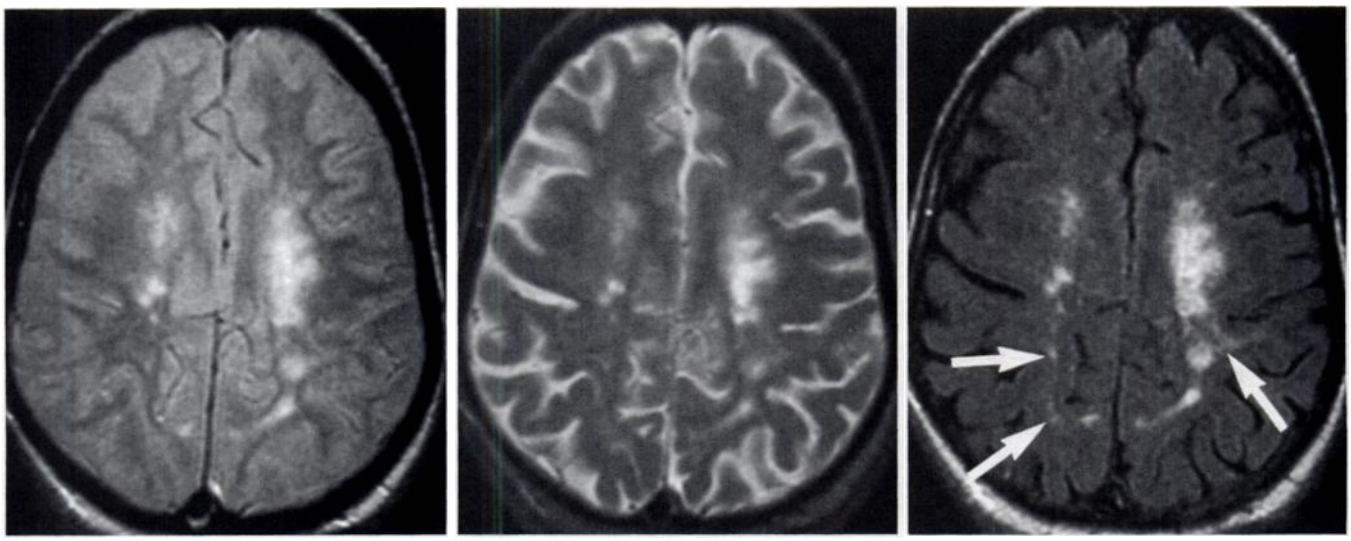

a. b. c.

Figure 5. Multiple sclerosis. **(a, b)** Conventional SE image (2,350/30, 80). **(c)** Fast FLAIR image (11,000/145/2,600). The fast FLAIR image gives much better lesion definition than either T2-weighted SE image, especially in the parietal white matter of the brain (arrows).

utes 8 seconds—a greater than 13-fold improvement in efficiency, given differences in image resolution (128 for original, 192 for fast FLAIR).

A chopping phase-encoding technique was qualitatively and quantitatively judged superior to four other phase-encoding techniques in its ability to minimize artifacts caused by using a RARE readout and by CSF inflow. We believe this phase-encoding technique may reduce RARE phase-encoding artifacts for two reasons. First, echoes with the greatest signal variation (echoes 1 and 16) from the signal found at the center of k space are placed farthest from this frequency space location. Second, the echo chopping effectively averages the signal amplitudes of the echoes that are being chopped while discarding the remaining signal modulation into the ghost removed from the image by using the extended field of view (no phase wrap). It is also believed that this phase-encoding technique reduces flow artifacts that result from interecho and interexcitation phase inconsistencies caused by the pulsatile nature of nonnulled CSF flow. Just as chopping averages signal amplitude differences, chopping is also believed to average phase values in the image and to discard the remaining phase differences into the unseen ghosts. A final artifact, areas of bright CSF seen in basal fast FLAIR sections of the brain, is an additional artifact caused by inflow of nonnulled CSF. This last artifact is not affected by phase-encoding choice.

Results were generated in a set of 41 consecutive patient studies subdivided into four patient groups (infarct, multiple sclerosis, small vessel ischemia, and miscellaneous). Quantitative analysis of all patient groups showed a significantly higher lesion-

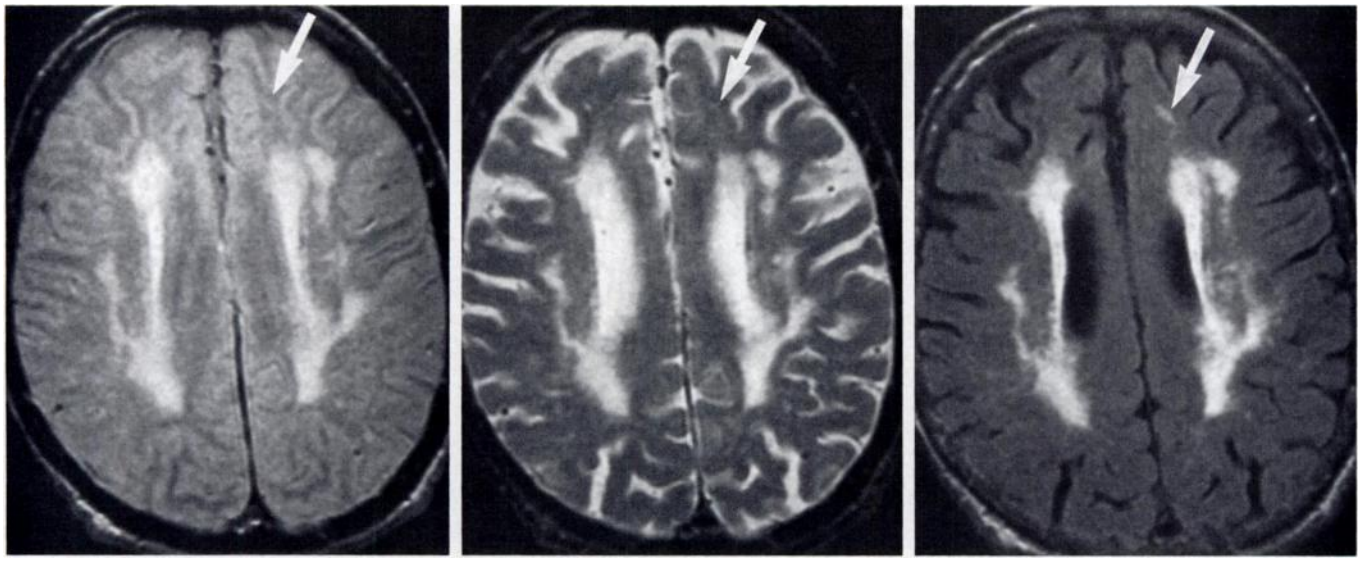

a. b. c.

Figure 6. Small vessel ischemia. **(a, b)** Conventional SE images (2,300/30, 80). **(c)** Fast FLAIR image (11,000/145/260) shows increased lesion conspicuity in the white matter of the left lobe. The fast FLAIR image also depicts an additional lesion in the left frontal lobe (arrow) not seen on either SE image.

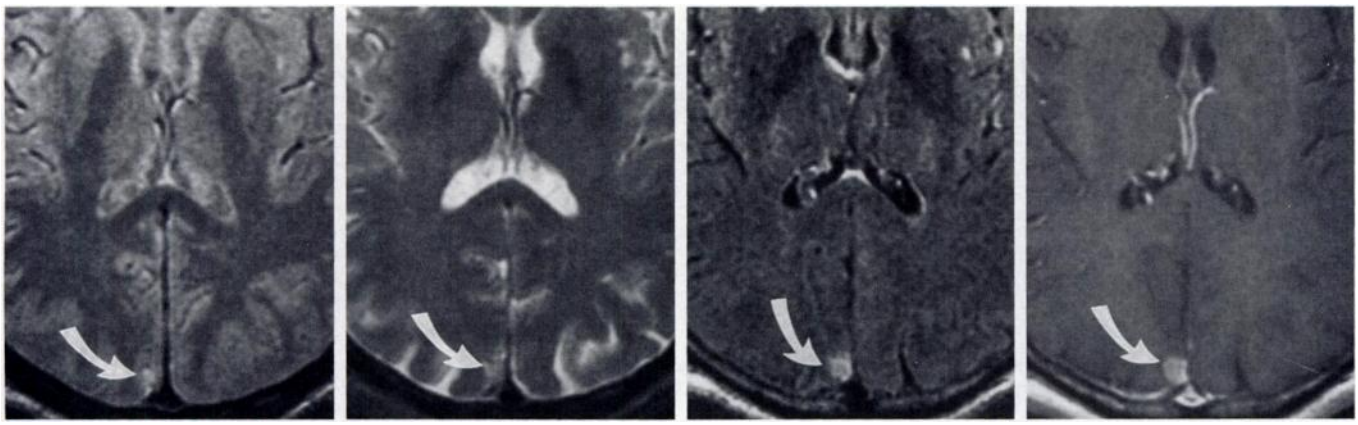

a. b. c. d.

Figure 7. Meningioma (arrow). **(a, b)** Conventional SE images (2,500/30, 80). The lesion is not readily seen. **(c)** Fast FLAIR image (11,000/145/2,600) shows the lesion, which was also seen on the next cephalic section. **(d)** The lesion was clearly seen with use of a T1-weighted SE sequence (650/29) after the administration of gadopentetate dimeglumine.

to-background contrast for fast FLAIR compared with either early- or late-echo long TR SE images. The lesion-to-background C/N of fast FLAIR was on average 84% higher than that of early-echo SE imaging and only slightly lower (12%) compared with an expected 29% C/N loss based on bandwidth differences for late-echo SE imaging. As a consequence of fast FLAIR eliminating the signal from CSF while preserving the signal for most lesions, the lesion-to-CSF C/N with fast FLAIR was on average 38 times greater than that with early-echo SE sequences and 75 times greater than that with late-echo SE sequences. Furthermore, the same TI provided effective CSF nulling for all patients and did not need to be adjusted on a patient-by-patient basis.

Results were also evaluated qualitatively by four neuroradiologists according to the standard radiologic criteria of lesion conspicuity, lesion detectability, and image artifact. The fast FLAIR sequence was rated statistically superior to the conventional dual-echo long TR SE sequence for conspicuity and detectability. Although fast FLAIR enabled detection of more lesions than T2-weighted SE imaging, the exact number of additional lesions detected cannot be quantified owing to differences in section sampling. The considerable increase in lesion-to-CSF contrast was thought to be one of the major factors in the improved lesion conspicuity with fast FLAIR.

Approximately 15% of the fast FLAIR evaluations—versus 5% of the gradient-moment-nulled T2-weighted SE evaluations—had one or more sections considered to be degraded by flow artifact. In general, this artifact occurred in areas of increased CSF flow and led to minor or moderate ghosting artifact due to the pulsatility of this flow. Based on previous results obtained with gradient-moment-nulled fast SE sequences (25), it is expected that such artifacts can be reduced by the incorporation of gradient moment nulling, particularly in the section-select direction.

In light of the marked improvement in lesion detectability, lesion conspicuity, and lesion-to-background and lesion-to-CSF contrast provided by the fast FLAIR sequence versus that obtained with conventional dual-echo long TR SE imaging,

one may question what the ultimate role of fast FLAIR will be. In one scenario, the fast FLAIR sequence may simply be appended to existing protocols for improved confidence in lesion detection. In a second scenario, fast FLAIR would replace the early-echo (proton-density–weighted) image of the long TR SE sequence and a RARE or fast SE technique would be used to acquire the late echo from this sequence, thus preserving gray and white matter anatomic detail. This second scenario, which uses only RARE-type readouts, would have potential drawbacks because of decreased sensitivity to hemosiderin (26,27) and increased fat signal and would preclude the ability to calculate T2 relaxation times. In addition, differential k-space effects would have to be recognized (9,28,29). Each of these may or may not be important. The major potential benefit of this scenario is the ability to efficiently image contiguous sections with increased sensitivity to abnormality, as demonstrated in this study. In an additional scenario, the unique signal characteristics of this FLAIR technique would be used in image processing applications, such as automated image segmentation of abnormality, possibly with thinner sections. Overall, as with any new sequence, large studies of patients will be needed to gain a more complete understanding of fast FLAIR. However, based on these preliminary results, we believe fast FLAIR is potentially useful. ■

Acknowledgments: We acknowledge the assistance of members of the Diagnostic Radiology Department at the Mayo Clinic, Rochester, Minn.

References

1. Brant-Zawadzki M, Norman D, Newton TH. Magnetic resonance imaging of the brain: the optimal screening technique. Radiology 1984; 152:71–77.
2. Hajnal JV, De Coene B, Lewis PD, et al. High signal regions in normal white matter shown by heavily T2-weighted CSF nulled IR sequences. J Comput Assist Tomogr 1992; 16:506–513.
3. De Coene B, Hajnal JV, Gatehouse P, et al. MR of the brain using fluid-attenuated inversion recovery (FLAIR) pulse sequences. AJNR 1992; 13:1555–1564.
4. White SJ, Hajnal JV, Young IA, Bydder GM. Use of fluid-attenuated inversion-recovery pulse sequences for imaging the spinal cord. Magn Reson Med 1992; 28:153–162.
5. Hajnal JV, De Coene B, Cowan FM, et al. Application of prolonged inversion and echo time inversion recovery (PIETIR) pulse sequences to diagnosis of disease of the brain (abstr). In: Book of abstracts: Society of Magnetic Resonance in Medicine 1992. Berkeley, Calif: Society of Magnetic Resonance in Medicine, 1992; 1007.
6. Hajnal JV, Kasuboski L, De Coene B, Young IR, Bydder GM. Imaging of the brain using PRe Inversion Multi Echo (PRIME) pulse sequences (abstr). In: Book of abstracts: Society of Magnetic Resonance in Medicine 1992. Berkeley, Calif: Society of Magnetic Resonance in Medicine, 1992; 1528.
7. De Coene B, Hajnal JV, Pennock JM, Bydder GM. MRI of the brain stem using fluid attenuated inversion recovery pulse sequences. Neuroradiology 1993; 35:327–331.
8. Hennig J, Nauerth A, Friedburg H. RARE imaging: a fast imaging method for clinical MR. Magn Reson Med 1986; 3:823–833.
9. Mulkern RV, Wong STS, Winalski C, Jolesz FA. Contrast manipulation and artifact assessment of 2D and 3D RARE sequences. Magn Reson Imaging 1990; 8:557–566.
10. Melki PS, Mulkern RV, Lawrence PP, Jolesz FA. Comparing the FAISE method with conventional dual-echo sequences. JMRI 1991; 1:319–326.
11. den Boer JA, Salverda P, Peters TR, Prevo RL. Multislice turbo-FLAIR in brain studies of multiple sclerosis (abstr). In: Book of abstracts: Society of Magnetic Resonance in Medicine 1993. Berkeley, Calif: Society of Magnetic Resonance in Medicine, 1993; 328.
12. Wehrli FW, Macfall JR, Newton TH. Parameters determining the appearance in NMR images. In: Newton TH, Potts DG, eds. Modern neuroradiology: advanced imaging techniques. San Anselmo, Calif: Claredal, 1983; 81–117.
13. Wood M, Bronskill M. MR desktop data. JMRI 1992; 2(S):13.
14. Bottomley PA, Foster TH, Argersinger RE, Pfeifer LM. A review of normal tissue hydrogen NMR relaxation times and relaxation mechanisms from 1–1000 MHz: dependence on tissue type, NMR frequency, temperature, species, excision, and age. Med Phys 1984; 11:425–488.
15. Park HW, Cho MH, Cho ZH. Time-multiplexed multislice inversion-recovery techniques for NMR imaging. Magn Reson Med 1985; 2:534–539.
16. Oshio K, Jolesz FA, Melki PS, Mulkern RV. T2-weighted thin-section imaging with the multislab three-dimensional RARE technique. JMRI 1991; 1:695–700.
17. Rydberg JN, Riederer SJ. Two-echo IR-RARE imaging with alternating echo times (abstr). JMRI 1992; 2(P):104.
18. Caspers JM, Rydberg JN, Krecke KN, Luetmer PH, Riederer SJ. Fast SE MR imaging of the larynx (abstr). Radiology 1993; 189(P):391.
19. Margosian P. Faster MR imaging: imaging with half the data (abstr). Book of abstracts: Society of Magnetic Resonance in Medicine 1985. Berkeley, Calif: Society of Magnetic Resonance in Medicine, 1985; 1024–1025.
20. MacFall JR, Pelc NJ, Vavrek RM. Correction of spatially dependent phase shifts for partial Fourier imaging. Magn Reson Imaging 1988; 6:143–155.
21. Riederer SJ, Tasciyan T, Farzaneh F, Lee JN, Wright RC, Herfkens RJ. MR fluoroscopy: technical feasibility. Magn Reson Med 1988; 8:1–15.
22. Melki PS, Mulkern RV, Panych LP, Jolesz FA. Replacing spin echo imaging with hybrid RARE sequences (abstr). Book of abstracts: Society of Magnetic Resonance in Medicine 1990. Berkeley, Calif: Society of Magnetic Resonance in Medicine, 1990; 1309.
23. Rosner B. Fundamentals of biostatistics. 3rd ed. Boston, Mass: Duxbury, 1990.
24. Kleinbaum DG, Kupper LL, Muller KE. Applied regression analysis and other multivariable methods. 2nd ed. Boston, Mass: PWS-Kent, 1988; 32.
25. Hinks RS, Constable RT. Flow compensation in fast spin echo imaging (abstr). Book of abstracts: Society of Magnetic Resonance in Medicine 1992. Berkeley, Calif: Society of Magnetic Resonance in Medicine, 1992; 891.
26. Jones KM, Mulkern RV, Mantello MT, et al. Brain hemorrhage: evaluation with fast spin-echo and conventional dual spin-echo images. Radiology 1992; 182:53–58.
27. Norbash AM, Glover GH, Enzmann DR. Intracerebral lesion contrast with spin-echo and fast spin-echo pulse sequences. Radiology 1992; 185:661–665.
28. Butts RK, Farzaneh F, Riederer SJ, Rydberg JN, Grimm RC. Intra-acquisition modification of pulse sequence parameters in MR imaging. Radiology 1991; 180:551–556.
29. Constable RT, Gore JC. The loss of small objects in variable TE imaging: implications for FSE, RARE, and EPI. Magn Res Med 1992; 28:9–24.